UNIVERSIDADE FEDERAL DO RIO GRANDE DO SUL

CURSO DE CIÊNCIAS BIOLÓGICAS

HENRIQUE CHAPOLA

ANÁLISE TRANSCRITÔMICA DE PERFIL METABÓLICO DE CÉLULAS-TRONCO MESENQUIMAIS ADIPOSAS EM HIPÓXIA E NORMÓXIA

Trabalho de Conclusão de Curso apresentado como requisito parcial para obtenção do título de bacharel em Ciências Biológicas da Universidade Federal do Rio Grande do Sul.

Orientador: Prof. Dr. Diego Bonatto

Co-orientadora:Msc. Joice de Faria Poloni

Estruturação e formatação nos conformes da *Journal of Cellular Biochemistry* (ISSN: 1097-4644)

Agradecimentos

Gostaria de agradecer a todos que contribuíram com a execução desse trabalho, não somente na parte técnica, prática e científica, mas também financeiramente, emocionalmente e espiritualmente.

Aos meus pais, João Sérgio Chapola e Maria das Graças Machado Chapola, muito obrigado por todo esforço para poder oferecer o melhor, em todos os sentidos. Junto aos meus irmãos, Eduardo Chapola e Fábio Chapola, obrigado pelo suporte, por acreditarem em mim e me encorajarem a eu seguir meu caminho, por mais saudades que eu deixe em vocês.

Á minha namorada e sua família, Juliana da Silva Luiz, Maria Denis da Silva Luiz e Nelson Machado Luiz, obrigado por me acolherem em sua casa e por me ajudarem todos os dias. Vocês são uma nova família que tenho aqui.

Ao professor Diego Bonatto, por me receber no grupo e apresentar o grande desafio que é a Biologia de Sistemas. O desafio foi essencial para meu autoconhecimento. A Joice de Faria Poloni pela co-orientação, sempre me ajudando nos momentos de maior dificuldade sem deixar de explorar o máximo do meu potencial.

Aos meus amigos do laboratório Beatriz dal Pont Duarte, Gabriel Baldissera, Gabrihel Stump Viegas, Kendi Nishino Miyamoto, Larissa Penna Siqueira, Raquel Calloni, obrigado também por me acolherem e por toda a verdadeira amizade.

Obrigado pelo amor!

Transcriptomic-based analysis of metabolic profile of adipose tissue-derived mesenchymal stem cells in hypoxia and normoxia

Henrique Chapola[a], Joice de Faria Poloni[a] and Diego Bonatto[a,*]

[a]Centro de Biotecnologia da Universidade Federal do Rio Grande do Sul, Departamento de Biologia Molecular e Biotecnologia, Universidade Federal do Rio Grande do Sul, Porto Alegre, RS – Brazil.

[*] To whom correspondence should be addressed:

Diego Bonatto

Centro de Biotecnologia da UFRGS - Sala 107

Departamento de Biologia Molecular e Biotecnologia

Universidade Federal do Rio Grande do Sul - UFRGS

Avenida Bento Gonçalves 9500 - Prédio 43421

Caixa Postal 15005

Porto Alegre – Rio Grande do Sul

BRAZIL

91509-900

Abstract

Adipose tissue-derived mesenchymal stem cells (hAMSC) are promisor therapeutic tool for regenerative medicine and chronic inflammatory diseases treatment due to its multipotency and immunomodulatory properties. However, to achieve the maximum potential of hAMSC in clinical trials, is necessary to understand the interplay of these cells with the environmental elements, such as the oxygen. Oxygen is a factor that participates in the regulation of metabolism and cell biology; however, how oxygen can affect hAMSC is not completely understood. In this work, a transcriptional analysis and a systems biology approaches was applied to evaluate the effects of atmospheric oxygen in hAMSC during 14 days of exposure, by comparing the initial time (21% [O_2] 0 d) and the final time (21% [O_2] 14d). Likewise, hAMSC were evaluated considering others oxygen concentrations, such as 5% (5% [O_2]) and 1% (1% [O_2]), which were compared to 21% [O_2] at final time (14d). Our data suggest that minor alterations in biological processes occur comparing between 21% [O_2] 14d and 21% [O_2] 0d, in term of differential expression. Genes related to cytokines and prostaglandins synthesis were upregulated suggesting an increased immunomodulatory effect over time. When was compared 21% [O_2] vs 1% [O_2] 14d, the normoxic condition showed downregulation of genes related to glycolysis and proliferation, as well as increased expression of genes associated with leucine catabolism, cholesterol synthesis, glutaminolysis, serine synthesis, oxidative stress, intrinsic apoptosis response and proliferation. The comparison with 5% [O_2] demonstrated that normoxic hASMC is under oxidative stress condition and activation of DNA

damage response. In conclusion, oxygen may have major effects in hAMSC at low concentration by shifting metabolism and the synthesis of molecules that coordinate alterations in regulation of hAMSC biology.

1. Introduction

Adipose tissue-derived mesenchymal stem cells (hAMSC) were first isolated and characterized as multipotent stromal cells found in white adipose tissue in 2002 (Zuk 2010). Since then, it was shown as a promising tool for regenerative medicine and against chronicle inflammatory diseases. These therapeutics applications are mostly due to the fact that hAMSC may differentiate mainly in osteogenic, chondrogenic, adipogenic lineages, although previous studies have shown wider differentiation potential (Wang et al. 2012, Pérez-Campo & Riancho 2015, Montzka et al. 2009). Another characteristic of hAMSC is this ability to secret of immunomodulatory molecules, such as interleukins, chemokines and prostaglandins (Wang et al. 2012). Furthermore, hAMSC are abundant cells, showing a concentration 500 fold greater than the bone marrow mesenchymal stem cells (BMMSC) and easily obtained through a simple puncture procedure (Fotia et al. 2015, Franco Lambert et al. 2009).

In order to exploit the maximum potential of immunomodulation and to optimize the differentiation capacity of hAMSC, is necessary to understand the mechanisms that regulate its molecular biology and biochemistry, and what are the best *in vitro* conditions to maintain them (Liu & Ma 2015).

A factor that influences stem cells is the oxygen concentration (Mohyeldin et al. 2010). In a physiological environment, hAMSC reside in a hypoxic niche with 2-8% oxygen concentration, which depends on the individual body mass

(Trayhurn 2013). The environmental hypoxic profile of hAMSC, similar to other stem cell types, makes them rely on anaerobic glycolysis, as well is maintained the multipotency and low proliferative capacity, in a quiescent state (Wang et al. 2005, Fotia et al. 2015). Nevertheless, oxidative phosphorylation and mitochondrial activity may increase depending oxygen availability, carrying metabolic alterations that contribute to differentiation, senescence and surviving of hAMSC (Atashi et al. 2015, Shyh-Chang et al. 2013).

An increase in mitochondria activity may lead to the production of reactive oxygen species (ROS), which are highly reactive and interfere in cells homeostasis (Atashi et al. 2015). Usually, the cells counteract high levels of ROS by producing antioxidants molecules and activating protective pathways;however, low levels of ROS have physiological implications in stem cells, specially by fine-tuning differentiation, proliferation and migration (Atashi et al. 2015, Maraldi et al. 2015).

Considering that hAMSC are routinely cultured in 21% [O_2], the major question is how different oxygen concentrations may interfere in hAMSC biochemistry and molecular biology. To address this question, transcriptome data and systems biology tools were employed to evaluate the influence of oxygen concentration in hAMSC.

2. Materials and methods

2.1 Differentially expressed genes selection

The transcriptome profile of hAMSC cultured in different oxygen concentrations was downloaded from the Gene Expression Omnibus database

using the package GEOquery implemented into R software (Sean & Meltzer 2007). The microarray matrix series GSE12884 held data of five different humans female donors derived hAMSC, aged between 22 and 44. As indicated by Pilgaard and colegues, the hAMSC were selected, seeded and after 24 hours of cultivation, were maintained at different oxygen concentrations for 14 days and medium was changed twice a week. Then, data was gathered at the beginning of conditioning (0d), and after it (14d) (Pilgaard et al. 2009).

The microarray quality was verified with the arrayQualityMetrics package, leaving four hAMSC donors-associated microarray data samples to further analysis (Kauffmann et al. 2009). In this study, the experimental group was considered the samples exposed to atmospheric oxygen at 14 days (21% [O_2] 14 d). The experimental group was compared with mild (5% [O_2] 14d), severe hypoxia (1% [O_2] 14d), and with the initial time (21% [O_2] 0d). This comparison was made using limma package (Ritchie et al. 2015) from R software, considering as parameters to cut-off $Log_2FC \geq |1|$, and false discovery rate (FDR) ≤ 0.05 to generate a list of differentially expressed genes (DEG). A table with all genes from each comparison, and every mentioned DEG in this manuscript is available in supplementary material (Supplementary Material 1).

2.2 Network interatomic data mining and visualization

The DEG lists were used as initial input for protein-protein interaction data mining at online software String 10.0 (Szklarczyk et al. 2015).

The parameters set were confidence degree 0.400, search options used were “database” and “experiments”, and maximum of 50 interactors shown in first shell.

After downloading the interatomic data, the networks were visualized, edited and further evaluated in software Cytoscape 2.8.3 (Shannon et al. 2003). Nodes were colored according to their Log_2FC. All nodes representing overexpressed DEG were colored with warm colors, whereas the nodes representing underexpressed DEG were colored with cold colors. Nodes that do not represent DEG were colored with gray (Fig.1, Fig. 2, Fig. 3A and C, Fig. 4A, C and E, Fig. 5A).

2.3 Cluster analysis

To assess the presence and number of clusters in the interatomic networks, the Cytoscape plugin AllegroMCODE was employed (Bader & Hogue 2003). Pre-processing parameters were the default settings, and post-processing parameters were fluffy node density equal to 0.1, and haircut enable. Only cluster with score ≥ 3 were selected for further gene ontology (GO) analysis (Fig. 3A and C, Fig. 4A, C and E, Fig. 5A). Clusters with similar GO results were merged.

2.4 Centrality analysis

To evaluate the most topological important nodes in the interatomic networks (nodes centrality), the Cytoscape plugin CentiScaPe 1.21 was used (Scardoni et al. 2009). The centralities analyzed were node and betweenness degree. Node degree evaluates the number of connections that each node have, whereas betweenness evaluates how many shortest paths between two different nodes in the network, passes through a referential node. The average scores were calculated, and the node with node degree and betweenness degree above the centrality score were selected as hub-bottlenecks (HB) (Fig.

2).HB nodes regulates many biological processes directly or indirectly by interacting with many nodes or connecting clusters (Scardoni & Laudanna 2012).

2.5 GO analysis

A GO analysis was performed in each identified clusters, using Cytoscape plugin BinGO 2.44 (Maere et al. 2005). The overrepresented GOs were evaluated by hypergeometric statistical test for quantitatively functional enrichment of GO according to whole annotations as a reference set. For multiple correction, the FDR was applied an adjusted p-value ≤ 0.05 as set. Just "biological processes" were selected to be analyzed (Fig. 3B and D, Fig. 4B, D and F, Fig. 5B). The lists with all genes, ontologies and corrected p-values are available as supplementary material (Supplementary Material 2, 3 and 4).

3. Results and Discussion

3.1 Comparison between hAMSC cultured in 21% [O_2]14d and in 21% [O_2] 0d

Comparing the transcriptome microarray data between 21% [O_2] 14 d and 21% [O_2] 0d, it was obtained 21 downregulated genes and 75 upregulated genes, and 13 genes only had statistical significance (Supplementary Material 1). From this DEG analysis, it was prospected interatomic data and generated a network with 222 nodes and 1112 edges. From all 66 DEG, 12 are underexpressed and 51 are overexpressed (Fig. 1A). Therewith, two clusters were further evaluated. Cluster 1 (Fig. 3A), with 667 edges, 18 overexpressed, 5 underexpressed and 115 non-differentially expressed genes, is mostly

associated with processes such as apoptosis, differentiation, proliferation and response to stress (Fig. 3B, Supplementary Material 2). Besides, the cluster 2, with 138 edges and 37 nodes of those being six overexpressed genes (Fig. 3C), is related to the response and cytokine production, inflammation and response to stress (Fig. 3D, Supplementary Material 2). In centrality analysis, 47 HB were observed, which only six were DEG, three overexpressed and three underexpressed (Fig. 2A).

3.1.1 Immunomodulatory genes expression increased in hAMSC at 14 d than at 0 d.

Upregulated genes related to immunomodulatory signaling were observed in cluster 2 (Fig. 2C), showing increased expression in hAMSC at 14 d. In addition, interleukin 6 (IL6) and interleukin 1 alpha (IL1A) were overexpressed, being these cytokines responsible for immunoregulatory processes, including immunosuppressive stimuli (Wang et al. 2014). Among other immunomodulatory molecules, there were upregulated chemokine genes C-C motif chemokine ligand 2 (CCL2) and C-C motif chemokine ligand 13 (CCL13)). These chemokines are chemoattractants, promoting dendritic cells migration, and both CCL2 and CCL13 expression may be induced by IL6 (Crop et al. 2010). Additionally, chemokine-binding protein 2 (CCBP2), a decoy receptor that sequestrate chemokines, inhibiting and preventing it action, is overexpressed (Lazennec & Richmond 2010).This suggests that CCL2 and CCL13 may participate in paracrine signaling in hAMSC, not autocrine.

In the main network (Fig. 1A), the prostaglandins metabolism was also found linked to immune systems. Genes related to arachidonic acid metabolism were overexpressed (phospholipase A2 group II A, (PLA2G2A), prostaglandin

synthase 1 (PTGS1) and prostaglandin I 2 synthase (PTGIS)) (Fig. 1A). Prostaglandins and prostacyclin are inflammatory agents that regulate vasodilatation and leukocyte adhesion (Ricciotti & Fitzgerald 2011). Furthermore, prostaglandins may have other functions than promote inflammation. Prostaglandins interact with other cells in adipose tissue. They promote development and maturation of pre-adipocytes and mature adipocytes, and this process may be a response to high levels of oxygen, since tissue oxygenation diminishes upon more developed adipose development, seen in obese people (Massiera 2003, Trayhurn 2013).

This data suggest that cell culture time and passage may induce an immunomodulatory transcriptomic profile, which may potentiate cytokines, chemokines and prostaglandins action (Wang et al. 2014, Lazennec & Richmond 2010).

3.1.2 Minor transcriptional changes occurs in hAMSC through time

Although immunomodulatory alterations have been seen, other biological processes are mostly represented by non-differentially expressed gene, or few DEG (Fig.1, Fig. 2A and B) that act in different pathways, playing roles in different processes, becoming difficult to stipulate alteration based on transcriptomic data.

The HB have central role in networks, and in this comparison, only six DEG were HB (Fig. 2A). Among the upregulated HB were Erb-B2 receptor tyrosine kinase 3 (ERBB3), a non-catalytic subunit of ERBb-Her receptors. It was observed that ERBB3 upregulation promoted glial-like differentiation of mesenchymal stem cells (MSC) (Mahay et al. 2008). But this was synergistically

achieved with other neurogenic factors that are not differentially expressed in this work. Another DEG HB upregulated is creatine kinase brain (CKB) which its expression was assessed in a comparison between primate adipose-tissue stem cells with and without telomerase, and CKB was upregulated in the non-transfected group, which had less osteogenic and proliferative capacity (Kang et al. 2004). The last upregulated HB is CCL2, and its participation in hAMSC was discussed in the previous topic.

Further, there were three underexpressed HB DEG, fibroblast growth factor receptor 3 (FGFR3), endothelin 1 (EDN1) e microtubule associated protein 1B (MAP1B) (Fig. 2B). The FGFR3 is a known promoter of chondrogenesis, but the lack of other genes expression to promote this action, especially fibroblast growth factor 18 (FGF18), do not contribute to the idea of reduction o chondrogenesis through cell culture time (Davidson et al. 2005). The EDN1 is described as a cytoprotector to MSC, promoting migration, cell viability and angiogenesis (Pourjafar et al. 2016). And MAP1B, a gene that encodes for a protein which regulates dynamically the cytoskeleton, and may exert a neurogenic-like effect in BMMSC (Montzka et al. 2009). Nevertheless, MAP1B activity depends on genes that do not exhibit differential expression. Additionally, the data between time comparison don’t agree with the promotion of differentiation since there was no differential expression of MSC markers (Calloni et al. 2013).

The data of this work shown lesser evidences of transcriptional changes in the regulation of biological processes of the cells, during the exposure of 14 days of the cells. This indicates that response to oxygen exposure may have a slow response, and 14 days is not enough, or that transcriptional response to

oxygen was effected during the period of 24 hours, when the cells were plated, before the gathering of transcriptional data (Pilgaard et al. 2009).

3.2 Comparison between hAMSC in 21% [O_2] and in 1% [O_2]

The microarray comparison between 21% [O_2] 14 d and 1% [O_2] 14 d resulted in a total of 1075 overexpressed genes, 991 underexpressed genes, and 2015 genes that were not differentially expressed. After interatomic data mining using DEG as input, a network with the total number of 1822 node, of those 366 are downregulated and 302 are upregulated DEG (Fig. 4A) was achieved.

A total of three clusters were found, after cluster analysis (Fig. 4A, C and E). The cluster 1 (Fig. 4A) that had 1477 nodes, which are 227 overexpressed genes and 279 were underexpressed, all connected through 34225 edges. This cluster is predominantly related to programmed cell death, cell cycle, response to oxidative stress, lipid metabolism and DNA damage stimulus (Fig 4B). Meanwhile, cluster 2 (Fig. 4C), with 12544 edges, had 1097 nodes, which 238 were downregulated and 175 were up, is more associated with proliferation, differentiation, apoptosis and chromatin organization (Fig. 4D). On the other hand, cluster 3 (Fig. 4E) was mainly associated with metabolism, such as glycolysis, aerobic respiration, tricarboxylic acid (TCA) cycle (Fig. 4F), and it had 165 upregulated and 164 downregulated DEG from a total of 953 nodes and 7152 edges. It was selected 371 node as HB, and 43 were downregulated just as 47 were upregulated (Fig. 2B).

3.2.1 Transcription data shown that TCA cycle activity is increased, while glycolysis is decreased hAMSC in 21% [O_2] compared to 1% [O_2]

The data related to hAMSC metabolism (Fig 4E and F) shown decreased expression of genes related to glycolysis and glucose transport, such as solute carrier family 2 member 14 (SLC2A14), solute carrier family 2 member 1 (SLC2A1), aldolase C (ALDOC),enolase 2 (ENO2),hexokinase 2 (HK2), 6-phosphofructo-2-kinase/fructose-2,6-bisphosphatase 2 (PFKFB2), 6-phosphofructo-2-kinase/fructose-2,6-bisphosphatase 3 (PFKFB3), 6-phosphofructo-2-kinase/fructose-2,6-bisphosphatase 4 (PFKFB4), phosphofructokinase, platelet (PFKP), phosphoglycerate mutase 2 (PGAM2) and pyruvate dehydrogenase kinase 3, PDK3) (Ochocki & Simon 2013). Meanwhile, the only genes that were upregulated are involved in gluconeogenesis. The phosphoenolpyruvate carboxykinase 2 (PCK2), which converts oxaloacetate to phosphoenolpyruvate (Mao et al. 2013), and glucose-6-phosphatase catalytic subunit 3 (G6PC3), that converts glucose-6-phosphate to glucose (Supplementary Material 1).

The results indicate an increased oxidative phosphorylation (Fig. 4E and F), because the PDK3 underexpression, an inhibitor of the conversion of pyruvate to acetyl-coA (De Miguel et al. 2015). Besides, upregulation in TCA cycle is mostly represented by overexpression of isocitrate desidrogenase 1, 3A e 3G (IDH1 (Fig. 2), IDH3A e IDH3G, respectively), that are responsible to perform the isocitrate conversion to alfa-ketoglutarate (αKG)(Ito & Suda 2014).

Other clues, such as metabolism of TCA intermediates (Fig. 4E and F) pointed an increased glutamonolysis in hAMSC in 21% [O_2] by overexpressing

glutamine channels (solute carrier family 38 member 1 (SLC38A1)) and glutaminase (GLS) and asparagine synthetase (ASNS). These genes encode for enzymes responsible for glutamine deamination, forming glutamate as product (Iwamoto & Mihara 2007, Ito & Suda 2014). In addition, a transaminase that performs the glutamate to oxaloacetate conversion, called glutamic-oxaloacetic transaminase 1 (GOT1) is upregulated. As consequence, oxaloacetate is pivotal to generates substrates to maintenance of the TCA cycle (Ito & Suda 2014).

It is known that hAMSC, as other stem cells, has low mitochondrial activity and relies on anaerobic glycolysis as an energy source in physiological concentrations. This metabolic status of stem cells helps the cells to regulate the proliferation, differentiation, self-renewal and surviving due to low exposure to stressors such ROS (Shyh-Chang & Ng 2017). Thus, hAMSC in 21% [O_2] show transcriptional differences that alter optimal stem cells metabolism, suggesting changes from its naïve characteristics at 21% [O2] (Shyh-Chang & Ng 2017).

3.2.2 Transcriptional alterations shown relationship between metabolism and increased replicative stress in hAMSC in 21% [O_2] compared to those in 1% [O_2]

Gene ontology and DEG in cluster 1 and 2 (Fig. 4A, B, C and D) shown that hAMSC in 21% [O_2] may proliferate less vigorously than in 1% [O_2]. Firstly, there is overexpression of a negative regulator of proliferation promyelocytic leukemia (PML), which promoted cell cycle arrest in BMMSC (Jie Sun, Shan Fu, Weijun Zhong 2013). Another fact is the downregulation of WNT1 inducible

signaling pathway protein 2 (WISP2), an adipokine that was shown to augment proliferation in precursor mesenchymal cells in vivo (Grünberg et al. 2017).

In this sense, transcriptional data represented in cluster 2 (Fig. 4C) where related to chromatin organization were present (Fig. 4D). Related to this, the DEG HB were upregulated, and they were represented by enhancer of zeste 2 Polycomb repressive complex 2 subunit (EZH2), a methyltrasferase catalytic subunit, and the histone chaperone anti-silencing function 1 homolog A (ASF1A) (Fig. 2B). Both DEG were mentioned in previous studies by their role in replicative stress response, preventing hematopoietic stem cells (HSC) from exhaustion when proliferation occurs in stressing conditions by regulating the chromatin state, leading to condensation (Kamminga et al. 2006, Khurana & Oberdoerffer 2015). Likewise, the overexpression of methionine adenosyltransferase 2A (MAT2A), which encodes the enzyme that performs conversion of methionine to S-adenosylmethionine (SAM), the main methyl donor to methylation reactions (Pérez-Campo & Riancho 2015). SAM is necessary to histones methyltransferase activity of EZH2 and may collaborate with replicative stress response (Kamminga et al. 2006).

Moreover, upregulated genes as phosphoserine aminotransferase 1 (PSAT1), phosphoglycerate dehydrogenase (PHGDH) and phosphoserine phosphatase (PSPH) propose higher serine synthesis. The serine metabolism present other roles than generated TCA cycle substrates, such as glycine and one carbon pathway substrates synthesis. At this point, the results suggest this alternative role of serine are represented by DEG upregulated methylenetetrahydrofolate dehydrogenase 2 (MTHFD2), that converts 5,10-methenyltetrahydrofolate to 5,10-methylenetetrahydrofolate, and serine

hydroxymethyltransferase 2 (SHMT2), which converts glycine and 5,10-methylenetetrahydrofolate to serine and tetrahydrofolate, although the Log_2FC for this gene was 0.68 (Supplementary Material 1). In both participation in glycine and one carbon pathway, serine metabolism may contribute indirectly the de novo synthesis of SAM, although this process is wider studied at cancer cells and embryoid bodies (Tedeschi et al. 2013).

The decreased proliferation, replicative stress, SAM generation and serine metabolism shown evidence of epigenetic changes. The epigenetic alterations, such as chromatin condensation, may contribute to loss of stemness of stem cells as consequence to 21% [O_2] exposure, as it changes expression of genes involved in stem state maintenance and differentiation (Shyh-Chang & Ng 2017).

3.2.3 Differentiation of hAMSC seems to be transcriptionally downregulated in 21% [O_2], than in 1% [O_2]

Although previous studies have shown differentiation occurring in an oxidative stress-dependent manner, this work did not have the same result (Zhou et al. 2015). In fact, some DEG related to cell differentiation were downregulated, such as peroxisome proliferator-activated receptor gamma (PPARG) and leptin (LEP), runt-related transcription factor 2 (RUNX2), proto-oncogene c-Kit (KIT) and chordin-like 2 (CHRDL2) which are involved in adipogenesis, osteogenesis and chondrogenesis, respectively. Furthermore, similarly to the comparison between 21% $[O]_2$ 14d and 21% $[O]_2$ 0 d, there was no difference in MSC markers expression (Calloni et al. 2013). This would means that neither in 21% [O_2] nor 1% [O_2] the hASMC developed greater

phenotypical changes or promoted cellular fate commitment in terms of transcription.

Among the mechanisms that regulate stemness and differentiation, one of the most discussed is the HIF pathway (Fotia et al. 2015). But contrary to what was expected, hypoxia inducible factor 1 alpha subunit (HIF1A) was overexpressed in normoxia. Although, a previous study shown that there was detectable HIF1A expression in BMMSC cultured under normoxia, and that this difference may be dependent on donors age (Palomäki et al. 2013). Though, unlike of the cited study, our data indicate that even with overexpressed HIF1A and degradation promoter DEG egl-9 family hypoxia inducible factor 1(EGLN1) downregulation, HIF pathway possibly is not active. Many genes regulated by HIF pathway, such as SLC2A14, SLC2A1, ALDOC, ENO2, HK2, PFKFB2, PFKFB3, PFKFB4, PFKP, PGAM2, PDK3, carbonic anhydrase 9 (CA9), LEP, vascular endothelial growth factor A (VEGFA), insulin-like growth factor 2 (IGF2), epidermal growth factor receptor (EGFR) were underexpressed in our results (Supplementary Material 1). According to our data, there might be two possibilities of HIF1A inactivation. Firstly the aryl hydrocarbon receptor nuclear translocator (ARNT), heterodimeric subunit necessary to downstream HIF pathways, is underexpressed (Mohyeldin et al. 2010). Additionally, with the overexpression, and presumed higher activity of IDH1 and PSAT1, more cytosolic αKG is being generated. The cytosolic αKG is a cofactor to HIF1A labeling and degradation, thus promoting increased HIF inhibition (Tedeschi et al. 2013, Ito & Suda 2014).

3.2.4 hAMSC shown oxidative stress, metabolism, and tumor protein 53 (TP53) related activity in 21% [O_2]

Some overexpressed DEG related to oxidative stress were found in cluster 1 (Fig. 4A and B). At first, the antioxidant gene NAD(P)H- quinone dehydrogenase 1 (NQO1), neutralize ROS by transferring two electrons to molecules such as quinones, quinoneimines and azo dyes and uses NADH or NADPH as hydride donors (Dinkova-Kostova & Talalay 2010). Both NADH and NADPH are related to DEG (IDH1, IDH3A, IDH3G, PHGDH, glucose-6-phosphate dehydrogenase (G6PDH) e phoshpogluconate dehydrogenase (PGD)) that enzymes produce them.

Additionally, the overexpressed gene 24-dehydrocholesterol reductase (DHCR24) is related to cholesterol and sterols synthesis, and it encoded an enzyme that utilize d-24 bounds of cholesterols as electron acceptor, performing an antioxidant activity (Kasz 2017). Interestingly, leucine catabolism may contribute to cholesterol synthesis products, as 3-hydroxy-3-methylglutaryl-coenzyme A (HMG-Coa), and accordingly to our data, this process might be stimulated in 21% [O_2] (Wortmann et al. 2012). There was overexpression of branched chain keto acid dehydrogenase E1 subunit beta (BCKDHB), related to the second and third step of all branched chain aminoacid catabolism (Zhao et al. 2016). Furthermore, isovaleryl-CoA dehydrogenase (IVD) and methylcrotonoyl-CoA carboxylase 2 (MCCC2), genes related only to leucine catabolism are upregulated along with leucine transporters solute carrier family 7 member 5 (SLC7A5) and solute carrier family 7 member 6 (SLC7A6) (Meierhofer et al. 2016, Chung et al. 2015). In this sense, it was proposed that leucine catabolism is related to the antioxidant activity of DHCR24.

Another overexpressed gene is thioredoxin-interacting protein (TXNIP), that was firstly studied its pro-oxidant action, by interacting with thioredoxin and

impairing antioxidant protection (Jung et al. 2013). However, it was observed in HSC that TXNIP interacts with MDM2 proto-oncogene (MDM2), which was underexpressed in the network (Fig. 1B, Supplementary Material 1), inhibiting it. This entails to TP53 degradation inhibition, leading to nuclear accumulation and transcriptional regulation of the oxidative stress (Jung et al. 2013).

In this sense, like TXNIP, NQO1 and DHCR24 positively regulates TP53 activity by preventing its degradation (Dinkova-Kostova & Talalay 2010, Kasz 2017). However, although TP53 was not a DEG, is a HB (Fig. 2B) with log_2FC equal to 0.913 (Supplementary Material 1).

3.2.5 ROS related pyroptosis is transcriptionally increased in hMSC 21% [O_2], compared to hAMSC in 1% [O_2]

The TP53 was suggested in the last topic to be stabilized by antioxidant enzymes. However, TP53 is related to activation of apoptosis, and as genes in all clusters suggest (Fig.4), apoptosis DEG as BH3 interacting domain death agonist (BID), cytochrome C, somatic (CYCS), are upregulated, and they promote intrinsic pathway (Wang & Youle 2009). Besides, caspase 1 (CASP1) is upregulated as well, and it promotes an alternative programmed cell death with inflammatory reaction called pyroptosis. A proteic complex called inflammasome activates the pyroptosis, and CASP1, is the effector subunit. When inflammasome is stimulated, CASP1 is released and cleaves pro-interleukin β, promoting inflammatory response (Shao et al. 2015). Between the stimuli that activate inflammasome there are mitochondrial damage and ROS. If redox balance suffers major alterations, TXNIP must act as an activator of inflammasome (Shao et al. 2015, Jung et al. 2013). The gene BCL2, apoptosis

regulator (BCL2), which is anti-apoptotic and inibit inflamassome, is underexpressed (Masters et al. 2012).

The current work suggests that hAMSC in 21% [O_2] have an increased tendency to pyroptosis, and must be related to its augmented mitochondrial activity and ROS-related defenses and apoptosis.

3.3 Comparison between hAMSC in 21% [O_2] and in 5% [O_2]

Microarray data comparison of hAMSC in 21% [O_2] 14 d and 5% [O_2] 14 d resulted in 106 upregulated genes, as just 15 were downregulated, and another 47 were only statistically significant, not reaching the minimum Log_2FC (Supplementary Material 1). The network generated from the prospection of the DEG had a total of 285 nodes connected by 1996 edges. It presented 66 of the DEG, separated in 11 underexpressed and 55 overexpressed genes (Fig. 1 C). According to gene ontology and cluster analysis, it was found one cluster (Fig. 5A), with 228 nodes and 1561 edges, of those 41 DEG, 36 were upregulated and five were downregulated. It is mostly related to response to stress, apoptosis, proliferation, response to oxygen levels and oxoacid metabolism (Fig. 5B, Supplementary Material 4). The centrality analysis highlighted 72 HB, but only nine were DEG overexpressed and none was underexpressed (Fig. 2C).

3.3.1 Transcription of glutaminolysis and serine synthesis genes are upregulated in hAMSC in 21% [O_2]

Accordingly to the networks, the metabolic profile of hAMSC in 21% [O_2] 14 d and 5% [O_2] 14 d have minor alteration, however, there are some similarities with the previous comparison of 1% [O_2]. The gluconeogenic gene

PCK2 is still upregulated, indication less glycolysis in 21% [O_2] (Fig. 5B, Supplementary Material 1). Additionally, glutaminolysis genes GOT1 and ASNS, as well as serine synthesis genes PHGDH, PSAT1 and PSPH are upregulated, which may generate more TCA cycle metabolites (Ito & Suda 2014). Previous studies corroborate with our data. They show that glucose consumption is more elevated in cells under 1.5% [O_2], as compared 5% [O_2] and 21% [O_2]. Glucose consumption was no different in 5% [O_2] and 21% [O_2]. Moreover, glutamate production was greater in 21% [O_2] than in 1,5% [O_2] and 5% [O_2] (Ejtehadifar et al. 2015).

3.3.2 Transcriptional ROS levels response is increased in hAMSC in 21% [O_2] than 5% [O_2], but it may being not extinguished

Another similarity between the comparisons with 21% [O_2], 5% [O_2] and 1% [O_2] is in the response to oxidative stress, where TXNIP and NQO1 overexpression remain. However, there was also overexpression of thioredoxin reductase 1 (TXNRD1), which participates in the thioredoxin cycle, reducing its oxidized form, thus promoting an antioxidant action. Although its activity can be prevented by TXNIP and this seems counterproductive, in biochemistry one has the idea that finely adjustment of metabolites may happen by investing energy in futile cycles (Quian & Beard 2006). Theoretically, this indicates that ROS levels are being adjusted, not only combated.

In this respect, our data show few differences between 21% [O_2] 14 d and 5% [O_2] 14 d (Fig. 5A and B), in relation to biological processes, in a similar way to what happened with the comparison between 21% [O_2] 14 d e 21% [O_2] 0 d (Fig. 2A and B). Nevertheless, besides to metabolic alterations, there were overexpression of HB growth arrest and DNA damage inducible alpha

(GADD45A) and DNA damage inducible transcript 3 (DDIT3) (Fig. 2C), which are related to cell cycle arrest and response to DNA and endoplasmic reticulum stress, pointing to effects of 21% [O_2] exposure (Zhan 2005, Jauhiainen et al. 2012).

4. Conclusion

In conclusion, oxygen plays a central role in the *in vitro* maintenance of hAMSC. It is an element of the environment that strongly is suggested to be controlled in the culture medium. Depending on the characteristics to be explored of the hAMSC, the adjustment of oxygen levels and their exposure time should be investigated and may enhance their proliferative, self-renewing or immunomodulatory abilities. It may should be considered to explore various levels of hypoxia since they can demonstrate a large difference in transcriptional response. It is possible to notice that the transcriptional response to oxygen level is much more delicate in hypoxic conditions when comparing the networks sizes and amount of DEG (Fig. 1). At that point, this work agrees with what other groups have already observed, demonstrating that little variation of oxygen concentrations is responsible for major changes (Ejtehadifar et al. 2015).

The data contribute to the relationship of metabolism and oxygen, especially in what it says mitochondrial activity. However, more studies are needed in order to better understand the function of metabolic pathways, such as serine, glutamate and cholesterol pathways, and this work indicates approaches to be taken.

5. Acknowledgments

This work was supported by the Conselho Nacional de Desenvolvimento Científico e Tecnológico (CNPq) grant 302969/2016-0. We thank Beatriz dal Pont Duarte, Kendi Nishino Miyamoto, Raquel Calloni and Bruno Cesár Feltes for helping in the analysis, R software utilization and contribution to discussion.

6. Conflicts of Interest

The authors declare no conflict of interest.

7. References

Atashi, F., Modarressi, A. & Pepper, M.S., 2015. The Role of Reactive Oxygen Species in Mesenchymal Stem Cell Adipogenic and Osteogenic Differentiation: A Review. *Stem Cells and Development*, 24(10), pp.1150–1163. Available at: http://online.liebertpub.com/doi/10.1089/scd.2014.0484.

Bader, G.D. & Hogue, C.W. V, 2003. An automated method for finding molecular complexes in large protein interaction networks. *BMC Bioinformatics*, 4, pp.1–27.

Calloni, R. et al., 2013. Reviewing and Updating the Major Molecular Markers for Stem Cells. *Stem Cells and Development*, 22(9), pp.1455–1476. Available at: http://online.liebertpub.com/doi/abs/10.1089/scd.2012.0637.

Chung, J. et al., 2015. The mTORC1/4E-BP pathway coordinates hemoglobin production with L-leucine availability. *Science signaling*, 8(372). Available at: http://www.ncbi.nlm.nih.gov/pubmed/25872869%5Cnhttp://www.pubmedcentral.nih.gov/articlerender.fcgi?artid=PMC4402725.

Crop, M.J. et al., 2010. Inflammatory conditions affect gene expression and function of human adipose tissue-derived mesenchymal stem cells. *Clinical and Experimental Immunology*, 162(3), pp.474–486.

Davidson, D. et al., 2005. Fibroblast growth factor (FGF) 18 signals through FGF receptor 3 to promote chondrogenesis. *Journal of Biological Chemistry*, 280(21), pp.20509–20515.

Dinkova-Kostova, A.T. & Talalay, P., 2010. NAD(P)H:quinone acceptor oxidoreductase 1 (NQO1), a multifunctional antioxidant enzyme and exceptionally versatile cytoprotector. *Archives Biochemistry Biophysics*, 501(1), pp.116–123.

Ejtehadifar, M. et al., 2015. The effect of hypoxia on mesenchymal stem cell biology. *Advanced Pharmaceutical Bulletin*, 5(2), pp.141–149. Available at: http://dx.doi.org/10.15171/apb.2015.021.

Fotia, C. et al., 2015. Hypoxia enhances proliferation and stemness of human adipose-derived mesenchymal stem cells. *Cytotechnology*, 67(6), pp.1073–1084. Available at: http://dx.doi.org/10.1007/s10616-014-9731-2.

Franco Lambert, A.P. et al., 2009. Differentiation of human adipose-derived adult stem cells into neuronal tissue: Does it work? *Differentiation*, 77(3), pp.221–228.

Grünberg, J.R. et al., 2017. Overexpressing the novel autocrine/endocrine adipokine WISP2 induces hyperplasia of the heart, white and brown adipose tissues and prevents insulin resistance. *Scientific Reports*, 7(February), p.43515. Available at: http://www.nature.com/articles/srep43515.

Ito, K. & Suda, T., 2014. Metabolic requirements for the maintenance of self-renewing stem cells. *Nature Reviews Molecular Cell Biology*, 15(4), pp.243–256.

Iwamoto, S. & Mihara, K., 2007. Mesenchymal cells regulate the response of acute lymphoblastic leukemia cells to asparaginase. *Journal of Clinical …*, 117(4), pp.1049–1057. Available at: http://www.jci.org/cgi/content/abstract/117/4/1049.

Jauhiainen, A. et al., 2012. Distinct cytoplasmic and nuclear functions of the stress induced protein DDIT3/CHOP/GADD153. *PLoS ONE*, 7(4), pp.1–9.

Jie Sun, Shan Fu, Weijun Zhong, H.H., 2013. PML overexpression inhibits proliferation and promotes the osteogenic differentiation of human mesenchymal stem cells. *Oncology Reports*, 30(6), pp.2785–2794.

Jung, H. et al., 2013. TXNIP maintains the hematopoietic cell pool by switching the function of p53 under oxidative stress. *Cell Metabolism*, 18(1), pp.75–85. Available at: http://dx.doi.org/10.1016/j.cmet.2013.06.002.

Kamminga, L.M. et al., 2006. The Polycomb group gene Ezh2 prevents hematopoietic stem cell exhaustion. *Blood*, 107(5), pp.2170–2179.

Kang, S.K. et al., 2004. Expression of Telomerase Extends the Lifespan and Enhances Osteogenic Differentiation of Adipose Tissue-Derived Stromal Cells. *Stem Cells*, 22(7), pp.1356–1372. Available at: http://doi.wiley.com/10.1634/stemcells.2004-0023.

Kasz, R., 2017. *Investigating DHCR24 as a protector against cellular stress : More than just a cholesterol- synthesising enzyme*.

Kauffmann, A., Gentleman, R. & Huber, W., 2009. arrayQualityMetrics - A bioconductor package for quality assessment of microarray data. *Bioinformatics*, 25(3), pp.415–416.

Khurana, S. & Oberdoerffer, P., 2015. Replication stress: A lifetime of epigenetic change. *Genes*, 6(3), pp.858–877.

Lazennec, G. & Richmond, A., 2010. Chemokines and chemokine receptors: new insights into cancer-related inflammation. *Trends in Molecular Medicine*, 16(3), pp.133–144. Available at: http://dx.doi.org/10.1016/j.molmed.2010.01.003.

Liu, Y. & Ma, T., 2015. Metabolic regulation of mesenchymal stem cell in expansion and therapeutic application. *Biotechnology Progress*, 31(2), pp.468–481.

Maere, S., Heymans, K. & Kuiper, M., 2005. BiNGO: a Cytoscape plugin to assess overrepresentation of gene ontology categories in biological networks. *Bioinformatics (Oxford, England)*, 21(16), pp.3448–9. Available at: http://www.ncbi.nlm.nih.gov/pubmed/15972284 [Accessed March 20, 2014].

Mahay, D., Terenghi, G. & Shawcross, S.G., 2008. Growth factors in mesenchymal stem cells following glial-cell differentiation. *Biotechnology and Applied Biochemistry*, 51(4), p.167. Available at: http://doi.wiley.com/10.1042/BA20070212.

Mao, P. et al., 2013. Mesenchymal glioma stem cells are maintained by activated glycolytic metabolism involving aldehyde dehydrogenase 1A3. *Proceedings of the National Academy of Sciences*, 110(21), pp.8644–8649.

Available at: http://www.pnas.org/cgi/doi/10.1073/pnas.1221478110.

Maraldi, T. et al., 2015. Reactive Oxygen Species in Stem Cells. *Oxidative Medicine and Cellular Longevity*, 2015, pp.1–2.

Massiera, F., 2003. Arachidonic acid and prostacyclin signaling promote adipose tissue development: a human health concern? *The Journal of Lipid Research*, 44(2), pp.271–279. Available at: http://www.jlr.org/cgi/doi/10.1194/jlr.M200346-JLR200.

Masters, S.L. et al., 2012. NLRP1 Inflammasome Activation Induces Pyroptosis of Hematopoietic Progenitor Cells. *Immunity*, 37(6), pp.1009–1023. Available at: http://dx.doi.org/10.1016/j.immuni.2012.08.027.

Meierhofer, D. et al., 2016. Ataxin-2 (Atxn2)-Knock-Out Mice Show Branched Chain Amino Acids and Fatty Acids Pathway Alterations. *Molecular & Cellular Proteomics*, 15(5), pp.1728–1739. Available at: http://www.mcponline.org/lookup/doi/10.1074/mcp.M115.056770.

De Miguel, M.P. et al., 2015. Cell metabolism under microenvironmental low oxygen tension levels in stemness, proliferation and pluripotency. *Current molecular medicine*, 15(4), pp.343–359.

Mohyeldin, A., Garzón-Muvdi, T. & Quiñones-Hinojosa, A., 2010. Oxygen in stem cell biology: a critical component of the stem cell niche. *Cell stem cell*, 7(2), pp.150–61.

Montzka, K. et al., 2009. Neural differentiation potential of human bone marrow-derived mesenchymal stromal cells: misleading marker gene expression. *BMC neuroscience*, 10(1), p.16. Available at:

http://bmcneurosci.biomedcentral.com/articles/10.1186/1471-2202-10-16.

Ochocki, J.D. & Simon, M.C., 2013. Nutrient-sensing pathways and metabolic regulation in stem cells. *Journal of Cell Biology*, 203(1), pp.23–33.

Palomäki, S. et al., 2013. HIF-1a is upregulated in human mesenchymal stem cells. *Stem Cells*, 31(9), pp.1902–1909.

Pérez-Campo, F.M. & Riancho, J.A., 2015. Epigenetic mechanisms regulating mesenchymal stem cell differentiation. *Current Genomics*, 16(6), pp.368–383. Available at: http://www.benthamdirect.org/pages/all_b_bypublication.php%5Cnhttp://ovidsp.ovid.com/ovidweb.cgi?T=JS&PAGE=reference&D=emed13&NEWS=N&AN=2015399168.

Pilgaard, L. et al., 2009. Transcriptional signature of human adipose tissue-derived stem cells (hASCs) preconditioned for chondrogenesis in hypoxic conditions. *Experimental Cell Research*, 315(11), pp.1937–1952. Available at: http://dx.doi.org/10.1016/j.yexcr.2009.01.020.

Pourjafar, M. et al., 2016. Cytoprotective effects of endothelin-1 on mesenchymal stem cells: an in vitro study. *Clinical and Experimental Pharmacology and Physiology*, 43(8), pp.769–776.

Quian, H. & Beard, D.A., 2006. Metabolic futile cycles and their functions: a systems analysis of energy and control. *Systems biology*, 153(4), pp.192–200.

Ricciotti, E. & Fitzgerald, G.A., 2011. Prostaglandins and inflammation. *Arteriosclerosis, Thrombosis, and Vascular Biology*, 31(5), pp.986–1000.

Ritchie, M.E. et al., 2015. limma powers differential expression analyses for RNA-sequencing and microarray studies. *Nucleic acids research*, 43(7), p.e47.

Scardoni, G. & Laudanna, C., 2012. Centralities Based Analysis of Complex Networks. *New frontiers in Graph Theory*, (2008). Available at: http://dx.doi.org/10.5772/35846.

Scardoni, G., Petterlini, M. & Laudanna, C., 2009. Analyzing biological network parameters with CentiScaPe. *Bioinformatics (Oxford, England)*, 25(21), pp.2857–9. Available at: http://www.pubmedcentral.nih.gov/articlerender.fcgi?artid=2781755&tool=pmcentrez&rendertype=abstract [Accessed March 21, 2014].

Sean, D. & Meltzer, P.S., 2007. GEOquery: A bridge between the Gene Expression Omnibus (GEO) and BioConductor. *Bioinformatics*, 23(14), pp.1846–1847.

Shannon, P. et al., 2003. Cytoscape: a software environment for integrated models of biomolecular interaction networks. *Genome Research*, 13(11), pp.2498–2504.

Shao, B.Z. et al., 2015. NLRP3 inflammasome and its inhibitors: A review. *Frontiers in Pharmacology*, 6(NOV), pp.1–9.

Shyh-Chang, N., Daley, G.Q. & Cantley, L.C., 2013. Stem cell metabolism in tissue development and aging. *Development (Cambridge, England)*, 140(12), pp.2535–47. Available at: http://www.ncbi.nlm.nih.gov/pubmed/23715547%5Cnhttp://www.pubmedcentral.nih.gov/articlerender.fcgi?artid=PMC3666381.

Shyh-Chang, N. & Ng, H.H., 2017. The metabolic programming of stem cells. *Genes and Development*, 31(4), pp.336–346.

Szklarczyk, D. et al., 2015. STRING v10: Protein-protein interaction networks, integrated over the tree of life. *Nucleic Acids Research*, 43(D1), pp.D447–D452.

Tedeschi, P.M. et al., 2013. Contribution of serine, folate and glycine metabolism to the ATP, NADPH and purine requirements of cancer cells. *Cell Death and Disease*, 4(10), p.e877. Available at: http://www.nature.com/doifinder/10.1038/cddis.2013.393.

Trayhurn, P., 2013. Hypoxia and Adipose Tissue Function and Dysfunction in Obesity. *Physiological Reviews*, 93(1), pp.1–21. Available at: http://physrev.physiology.org/cgi/doi/10.1152/physrev.00017.2012.

Wang, C. & Youle, R.J., 2009. The Role of Mitochondria in Apoptosis. *Annual Review of Genetics*, 43, pp.95–118.

Wang, D.W. et al., 2005. Influence of oxygen on the proliferation and metabolism of adipose derived adult stem cells. *Journal of Cellular Physiology*, 204(1), pp.184–191.

Wang, S., Qu, X. & Zhao, R.C., 2012. Clinical applications of mesenchymal stem cells. *Journal of hematology & oncology*, 5(1), p.19. Available at: http://www.jhoonline.org/content/5/1/19.

Wang, Y. et al., 2014. Plasticity of mesenchymal stem cells in immunomodulation: pathological and therapeutic implications. *Nature Immunology*, 15(11), pp.1009–1016. Available at:

http://www.nature.com/doifinder/10.1038/ni.3002.

Wortmann, S.B. et al., 2012. The 3-methylglutaconic acidurias: What's new? *Journal of Inherited Metabolic Disease*, 35(1), pp.13–22.

Zhan, Q., 2005. Gadd45a, a p53- and BRCA1-regulated stress protein, in cellular response to DNA damage. *Mutation Research - Fundamental and Molecular Mechanisms of Mutagenesis*, 569(1–2), pp.133–143.

Zhao, X. et al., 2016. The Relationship between Branched-Chain Amino Acid Related Metabolomic Signature and Insulin Resistance: A Systematic Review. *Journal of Diabetes Research*, 2016.

Zhou, D., Shao, L. & Spitz, D.R., 2015. *Reactive Oxygen Species in Normal and Tumor Stem Cells*,

Zuk, P.A., 2010. The Adipose-derived Stem Cell: Looking Back and Looking Ahead. *Molecular Biology of the Cell*, 21(22), pp.1783–1787.

8. Figures:

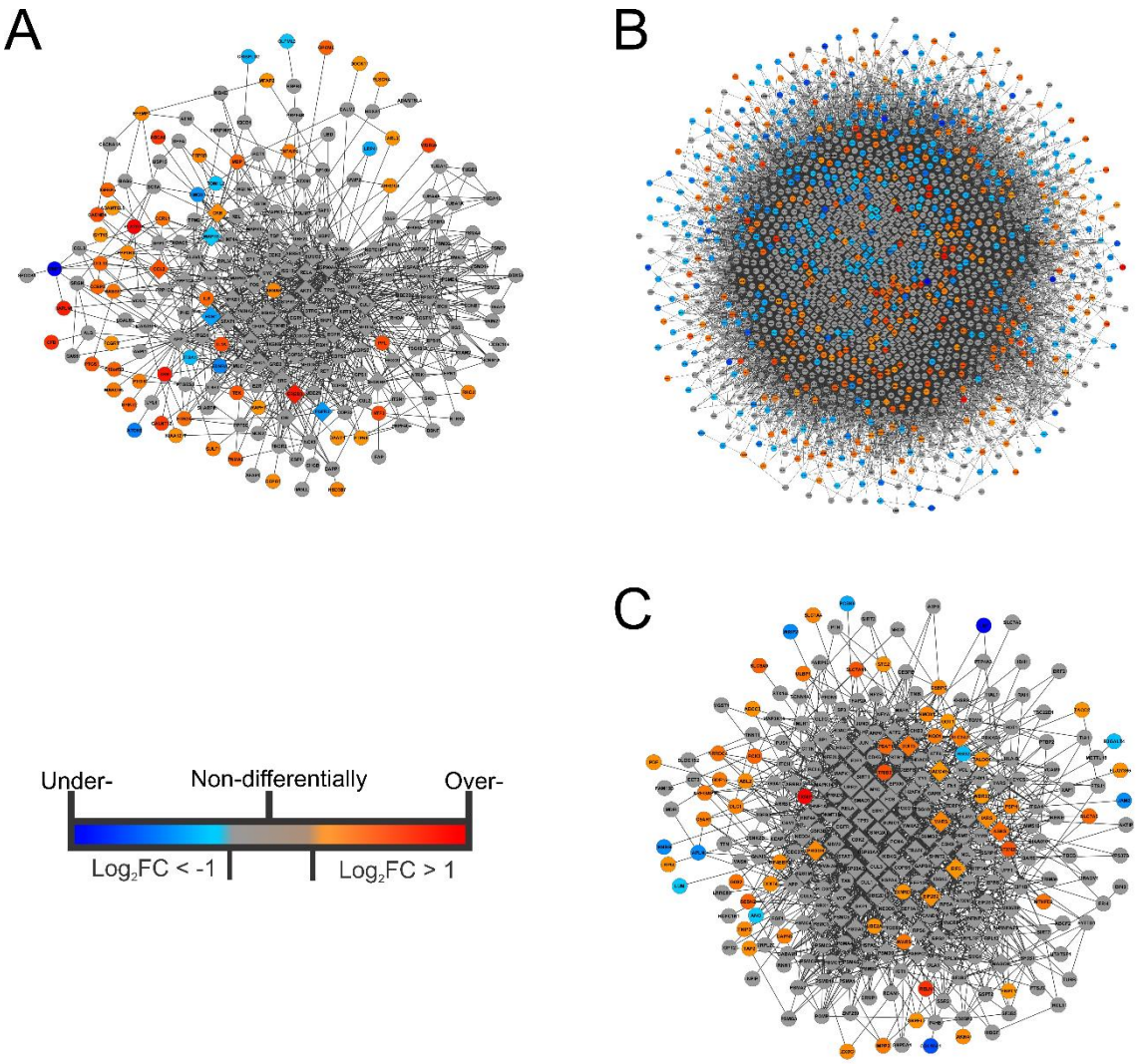

Fig. 1: Whole networks generated in Cytoscape 2.8.3. (A) Network resulted from the 21% [O_2] 14 d and 21% [O_2] 0 d comparison, with 1112 edge, 222 node. From all nodes, 12 are underexpressed DEG and 51 are overexpressed. (B) Network from the comparison between 21% [O_2] 14d and 1% [O_2] 14d, with 44425 edge, 1822 node, with 668 were DEG, divided in 366 downregulated and 302 upregulated. (C) Network resulted from the comparison between 21% [O_2] 14d and 5% [O_2] 14d, with 1996 edge connecting a total of 285 nodes, 11 underexpressed DEG and 55 overexpressed.

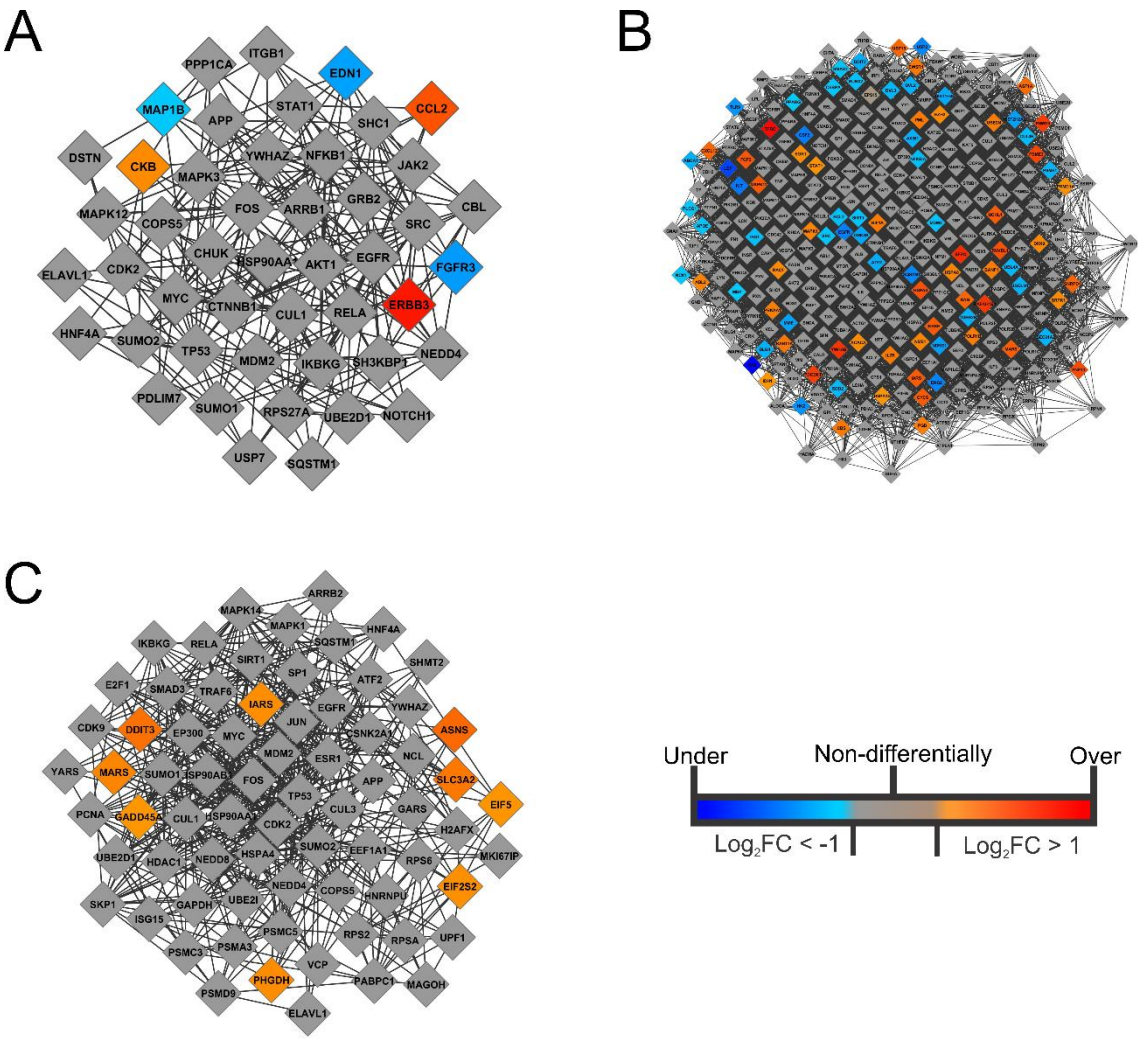

Fig. 2: Sub-network showing all HB, represented in the networks as diamond-shaped nodes. (A) Total of 47 HB from 21% [O_2] 14 d vs. 21% [O_2] 0 d comparison, of which 6 are DEG, being three upregulated and three down. (B) From 21% [O_2] 14 d vs. 1% [O_2] comparison, 371 HB were selected, 90 are DEG, as 43 were downregulated and 47 were upregulated. (C) The 21% [O_2] 14 d vs. 5% [O_2] 14 d comparison had a total of 72 HB, of which nine are overexpressed DEG.

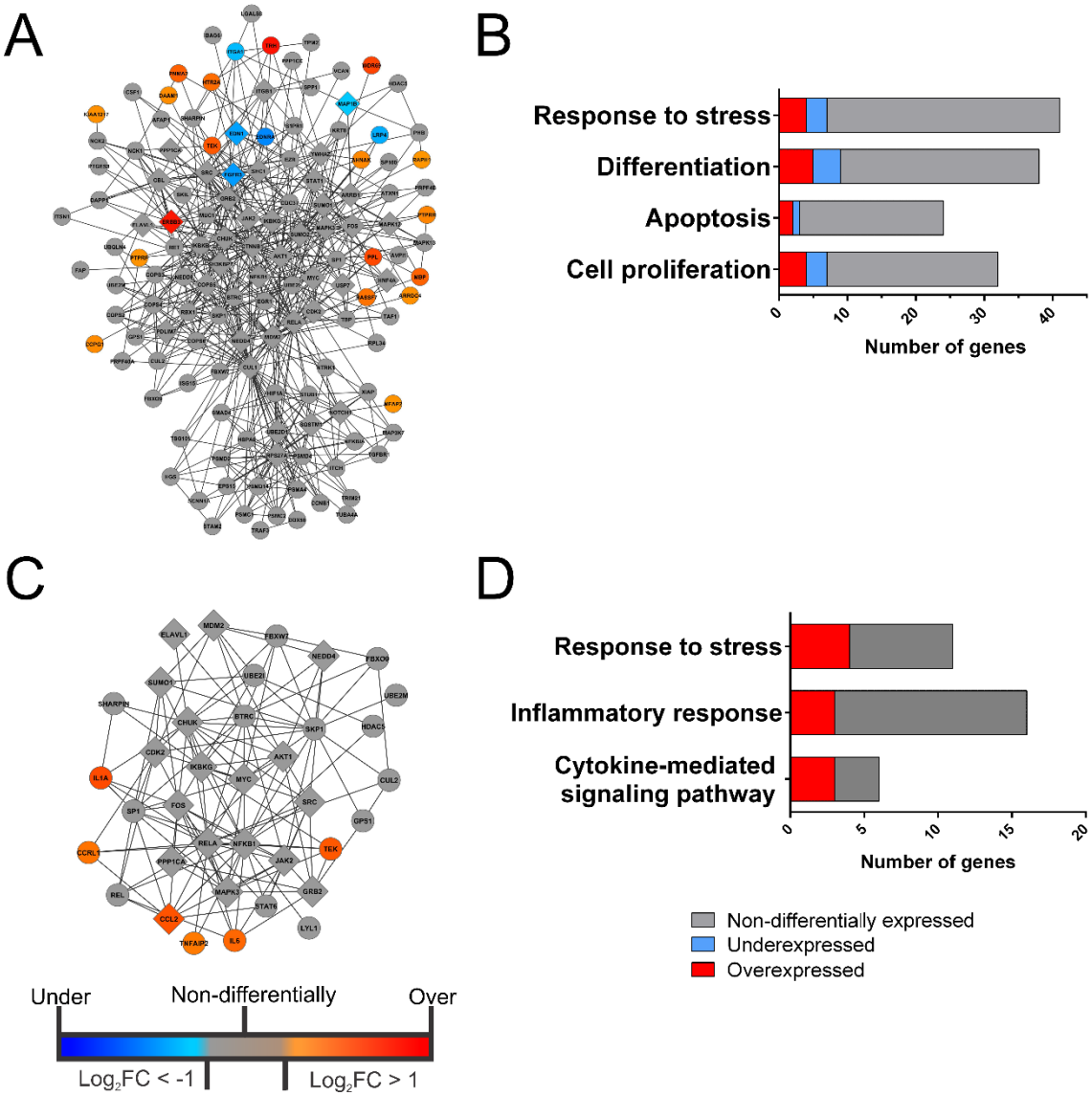

Fig. 3: Clusters and gene ontologies with number of genes, from the time comparison network (Fig. 1 A). (A) Cluster 1, with 664 edges, 138 nodes and 24 DEG, 18 overexpressed and five underexpressed. (C) Cluster 2, with 138 edges, 37 nodes and 6 DEG, all overexpressed. On right side, the respective gene ontology associated with each cluster (B and D), with number of genes associated to each process. Adjusted p-value < 0.001 for all ontologies (Supplementary Material 2).

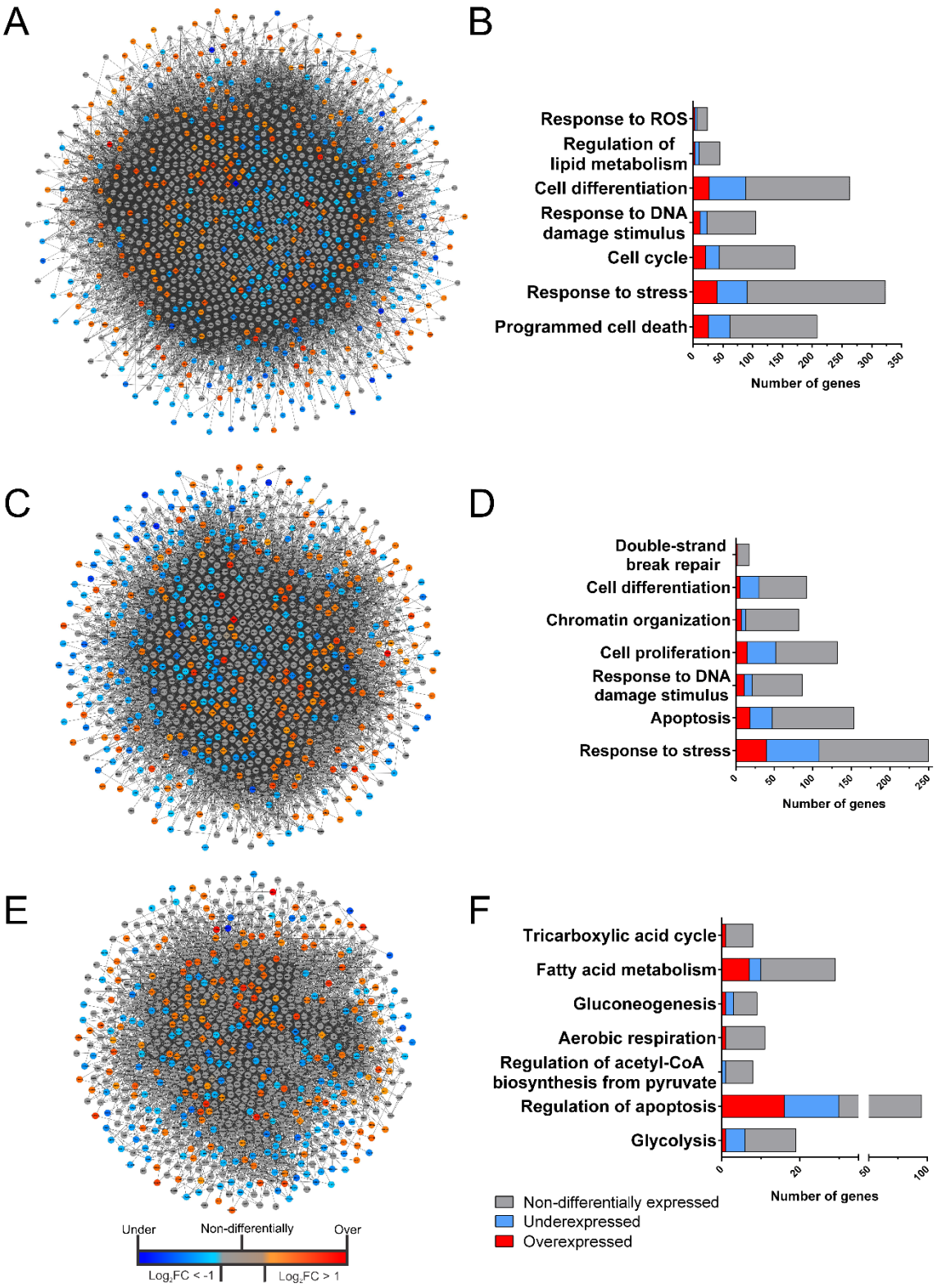

Fig. 4: Clusters and gene ontologies with number of genes, from the 21% [O_2] and 1% [O_2] comparison network (Fig. 1 B). (A) Cluster 1, with 34225 edges edges, 1477 nodes and 506 DEG, of which 227 are upregulated and 279 are

downregulated. (C) Cluster 2, with 12544 edges, 1097 nodes, 238 downregulated DEG and 175 upregulated. (E) Cluster 3, with 7152 edges, 953 nodes, of which 165 are overexpressed genes and 164 are underexpressed. On right side, the respective gene ontology associated with each cluster (B, D and F), and representing the number of genes involved with each process. Adjusted p-value < 0.001 for all ontologies (Supplementary Material 3).

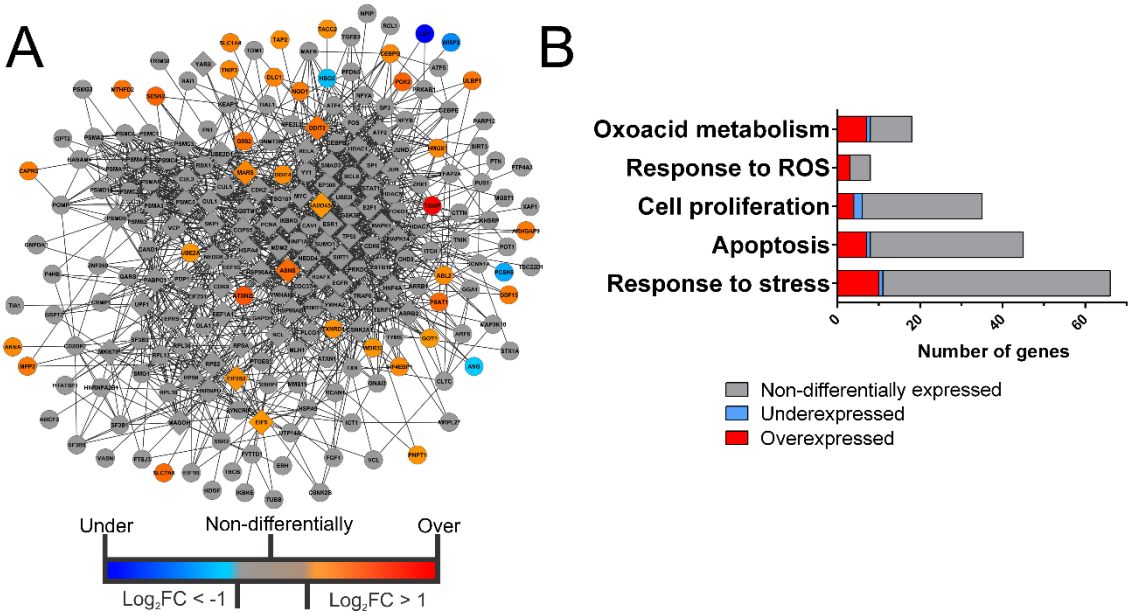

Fig. 5: Clusters and gene ontologies with number of genes, from the 21% [O_2] and 5% [O_2] comparison network (Fig. 1C). (A) Cluster 1, with 1561 edges, 228 nodes and 41 DEG, of which 36 are overexpressed and five are under. (B) Gene ontologies associated to cluster 1, adjusted p-value < 0,001 for all ontologies (Supplementary Material 4).

9. Supplementary Material

Supplementary Material 1: Whole gene expression tables, showing genes names (ID), Log_2FC and adjusted p-value. Each sheet contains the comparative data from each situation. The name of the sheet represent which comparison

are the data. Last sheet have separated all genes mentioned in this manuscript. Comparison names are above it respective table.

Supplementary Material 2: Whole gene ontology results from the clusters in comparison 21% [O_2] 14 d vs. 21% [O_2] 0 d Gene ontology results containing gene ontologies, adjusted p-value, number of nodes present in the cluster that are involved with the specific ontology (x), total identified proteins for each ontology (n) and the list of set genes related to the ontology.

Supplementary Material 3: Whole gene ontology results from the clusters in comparison 21% [O_2] 14 d vs. 1% [O_2] 14 d. Gene ontology results containing gene ontologies, adjusted p-value, number of nodes present in the cluster that are involved with the specific ontology (x), total identified proteins for each ontology (n) and the list of set genes related to the ontology.

Supplementary Material 4: Whole gene ontology results from the clusters in comparison 21% [O_2] 14 d vs. 5% [O_2] 14 d. Gene ontology results containing gene ontologies, adjusted p-value, number of nodes present in the cluster that are involved with the specific ontology (x), total identified proteins for each ontology (n) and the list of set genes related to the ontology.